

Scalable Power System Line Upgrade Planning With Policy Constraints: A “Branch and Benders” Approach

Sandro Merkli^{*†}, Roy S. Smith[†]

Latest revision: January 2022

Abstract

The integration of more renewable energy sources into the power system is presenting system operators with various challenges. At the distribution system level, voltage magnitudes that violate operating limits near large photovoltaic installations have been observed. While these issues can be partially mitigated with more advanced control, hardware upgrades are required at some point. This work presents a scalable, optimization-based approach for deciding which lines in a network to upgrade. Compared to existing approaches, it explicitly takes the operating policy of the system into account and provides both reasonable solutions in short computation times as well as globally optimal solutions when run to completion. Compared to earlier work on the same topic, an extended computational approach is taken that can simultaneously optimize for many load scenarios across arbitrary configurations of machines and CPU cores per machine in a scalable manner by using the Benders decomposition. In addition to the theory, numerical experiments are presented along with a discussion of the scaling properties of the Benders-based approach, giving potential users a better basis to decide whether their problem is big enough for the approach to make sense.

1 Introduction

The share of renewable energy sources is increasing in power systems [1]. While newly deployed renewables make power generation more sustainable, they also present challenges to power system operators. One such challenge is voltage magnitude rise due to photovoltaic systems in low to medium voltage distribution networks [2]. Because the lines in such networks have non-negligible resistance, voltage differences between buses become relevant. If the power in-feed due to local generation is too high, voltage magnitudes can exceed the operating limits near the feed-in point. In order to avoid damage to end user devices, steps have to be taken to mitigate such overvoltage occurrences.

System operators can either change the operating policy of the system or perform upgrades to the system itself. Examples of the former include curtailment of the photovoltaic systems [3] and changes in on-load tap changing (OLTC) transformer control schemes. Such changes tend to be less costly to implement than system hardware upgrades. On the other hand, curtailment is not desirable as valuable renewable energy remains unused. System hardware upgrade possibilities include energy storage devices, OLTC hardware upgrades or power line upgrades. In this work, only power line upgrades are considered since they are the most readily available at the time of this writing.

The general optimization problem of deciding which components of a power system to upgrade is hard to solve: The question whether an admissible operating point exists for a given AC power system and load pattern is already NP-hard to answer in general [4]. For line upgrades in particular, an additional difficulty stems from the fact that line hardware is typically available for purchase with fixed increments in admittance. Even if line hardware was more available with user-specifiable admittance, the cost of upgrading a line is in practice dominated by the construction work required for the upgrade and not by the line admittance

^{*}embotech AG, Giessereistrasse 18, 8005 Zurich

[†]Automatic Control Lab, ETH Zurich, Physikstrasse 3, 8092 Zurich {smerkli, rsmith}@control.ee.ethz.ch

cost. In order to model this cost accurately, integrality constraints have to be added to the problem, further increasing its difficulty.

These complicating factors make the power system line upgrade problem intractable to solve in general. Existing methods therefore take steps to simplify the problem in various ways. In terms of objective, most existing work minimizes upgrade or upgrade plus operation cost for a given scenario [5, 6]. One line of research then approximates the more accurate AC model by a computationally tractable DC model consisting of linear equations [7]. The resulting mixed-integer linear problem, while still NP-hard, can usually be solved in a reasonable amount of time with state-of-the-art optimization solvers. The caveat in this approach is that the result is not guaranteed to be a viable solution to the full AC model of the system, let alone practically deployable. A related approach uses convex relaxations of the power flow equations, such as the ones presented in [8, 9], to create formulations that share the same caveat, but provide the added benefit of a lower bound on the number of line upgrades required [10]. A different approach is to apply heuristic methods for finding reasonable solutions to the problem [6, 11]. It has been shown that these methods find reasonably good solutions to practical problems, but they do not provide any lower bounds on the objective value.

The method presented in this paper combines the lower-bounding and heuristic methods by means of a Branch-and-Bound procedure. This procedure is then extended with constraint generation and a distributed optimization based on the Benders decomposition. The result is an algorithm that can both find practically deployable solutions to the line upgrade problem in reasonable computation times as well as certified globally optimal solutions if it is run to termination. The use of the Benders decomposition algorithm for solving relaxations enables the method to trivially be able to make use of a number of parallel computing agents up to the number of scenarios considered in the optimization. Since the most computationally demanding parts of the algorithm can be run in parallel this way, computation times are almost linearly improved by the addition of more parallel agents.

This scalability in the number of scenarios is a big step towards practical applicability of sampling-based methods [12–14] for power system planning problems.

1.1 Contribution

The method presented improves on the state of the art in the following aspects:

- a) The operating policy used in practice is integrated directly into the optimization problem formulation. This guarantees that the selected upgrade configuration is also feasible when deployed, while existing approaches at best guarantee that a feasible operating point exists.
- b) The algorithm is compatible with existing heuristics for finding useful solutions (upper bounds) and can make use of existing convex relaxations.
- c) Multiple scenarios can be specified instead of a single worst-case scenario and the system topology can be optimized over all of them jointly.

Compared to our earlier conference paper on the same topic [15], this work includes the following extensions:

- 1) A detailed treatment of the reformulation of the original problem into a mixed-integer quadratically constrained quadratic problem (MI-QCQP) is given.
- 2) An approach based on the Benders decomposition is applied to the mixed-integer semidefinite (MI-SDP) relaxations arising in the Branch-and-Bound procedure and integrated with the latter, making the procedure scalable and amenable to parallelization.
- 3) Numerical experiments are presented that demonstrate how the described approach benefits from parallelism.

1.2 Contents

Section 2 outlines the model used in this work. Section 3 presents the problem formulation and its reformulation into a mixed-integer quadratic problem with policy constraints. Section 4 then presents the main algorithm. Numerical experiments are presented and discussed in Section 5.

2 Modeling

In the following, \bar{x} will be used to denote the element-wise complex conjugate of a variable x . The operators $\text{Re}(x)$ and $\text{Im}(x)$ are used to denote the real and imaginary parts of variable x . The operator $x \cdot y$ is used in some places to denote the product xy of scalars x and y to improve readability.

2.1 Power system

A power system with N buses and L lines is modeled using the bus injection model of the AC power flow equations,

$$s = \text{diag}(v) \overline{Y} v, \quad (1)$$

where $s \in \mathbb{C}^N$ and $v \in \mathbb{C}^N$ represent the complex powers and voltages at the buses of the system. The Laplacian $Y \in \mathbb{C}^{N \times N}$ contains all information about the system topology considered in this work:

$$Y_{jl} := \begin{cases} y_{jl} & \text{if } j \neq l, \\ -\sum_{k=1, k \neq j}^N y_{jk} & \text{if } j = l, \end{cases} \quad (2)$$

where y_{jl} is the complex admittance of the line between buses j and l . Shunt admittances are not included in the model for notational simplicity, but could be added by modifying equations (2), (4) and the reformulation in Section 3 accordingly.

2.2 Operating limits

All buses are assumed to have voltage magnitude limits as well as power limits:

$$\begin{aligned} v_{\min,j} &\leq |v_j| \leq v_{\max,j}, \\ p_{\min,j} &\leq \text{Re}(s_j) \leq p_{\max,j}, \\ q_{\min,j} &\leq \text{Im}(s_j) \leq q_{\max,j}, \end{aligned} \quad (3)$$

By making different subsets of the above constraints tight (i.e. the minimum value equal to the maximum value), one can model PV, PQ as well as slack buses in a unified manner. For example, a PQ load could have the latter two limits tight and the voltage magnitude constrained to $[0.9, 1.1]$ per unit. For the slack bus, the voltage magnitude would be fixed but the other two limits would not be present. The thermal limits on power lines are represented using a current-based formulation:

$$|Y_{jl}| \cdot |v_j - v_l| \leq I_{\max,jl}. \quad (4)$$

Note that other convex constraints, such as apparent power limits on generators, can be included in the formulation if desired and the method presented here is still applicable.

2.3 Violating scenarios

Similar to other work in the field, we take the approach of minimizing the cost of upgrades. However, instead of looking at only a worst case, we introduce the concept of *violating scenarios*. We assume the availability of K separate system steady-state scenarios, indexed with the letter k , in the form of powers and voltages (s^k, v^k) along with power limit data $p_{\min}^k, p_{\max}^k, q_{\min}^k$ and q_{\max}^k . These scenarios can come from past measurements, simulations of hypothetical scenarios or also from worst-case studies. The method presented here is scalable in the number of such scenarios. It will find a set of upgrades that, combined with the operating policy introduced in the next section, leads to no constraint violations in all scenarios. If no such set exists, the method will certify that this is the case.

2.4 Operating policies

As mentioned in the introduction, it has been shown to be hard to decide whether a power dispatch exists that satisfies the Kirchhoff equations (1) as well as the operating constraints (3), (4) for a given load pattern. Fortunately, what is relevant in practice to a system operator is less whether a solution exists in theory, but rather whether they can find it with their system operating policy. We model this policy as a function of the system topology Y and the operating limits specific to the scenario:

$$(\tilde{s}^k, \tilde{v}^k) = g(Y, \text{limits}^k), \quad (5)$$

where “limits^k” includes the data v_{\max} , v_{\min} , I_{\max} , p_{\min}^k , p_{\max}^k , q_{\min}^k and q_{\max}^k . This work assumes that the voltage and line current limits are the same across all scenarios whereas the active and reactive power limits may be different. The policy function can choose values for the powers and voltages within the given limits, leading to new vectors $(\tilde{s}^k, \tilde{v}^k)$. This is done to model the fact that, given a different topology, a different dispatch might have been chosen. Examples of such policy functions are an AC economic dispatch or local controllers. The assumptions made about g are that it is tractable to evaluate and that the $(\tilde{s}^k, \tilde{v}^k)$ returned by (5) satisfy (1).

2.5 Line upgrades

Line upgrades are modeled as changes in admittance and can be formulated in a vectorized manner,

$$Y_{\text{upg}}(a) = Y + \sum_{i=1}^{n_u} (a_i \cdot \Delta Y_i), \quad (6)$$

where $a_i \in \{0, 1\}$ indicates whether the upgrade is performed (1) or not (0), the constant matrix ΔY_i determines the change from the original system topology Y if upgrade i is performed and n_u is the total number of such upgrade possibilities. Constraints on the upgrade combinations are expressed as a separate set of linear constraints,

$$Aa \leq b. \quad (7)$$

This set of constraints is used to ensure that at most one type of line upgrade is performed per line. If a line upgrade is performed, its current limit can also change,

$$I_{\max, \text{upg}, jl} = I_{\max, jl} + \sum_{i \in \mathcal{U}_{jl}} (a_i \cdot \Delta I_{jl, i}), \quad (8)$$

where \mathcal{U}_{jl} is the set of indexes i which refer to upgrade choices that affect the line from bus j to bus l .

3 Upgrade problem and Big-M formulation

In this section, the upgrade problem is formulated mathematically. It is then brought into a standard MI-QCQP form, which in turn will admit an MI-SDP relaxation in Section 4.

3.1 Problem formulation and standard form

The system upgrade problem is given as follows:

Problem U:

$$\underset{a, \tilde{s}^k, \tilde{v}^k}{\text{minimize}} \quad 1^T a \quad (\text{U.1})$$

$$\text{subject to} \quad a \in \{0, 1\}^{n_u}, \quad (\text{U.2})$$

$$(5), (6), (7), (8), \quad (\text{U.3})$$

$$(1), (3) \text{ for } \tilde{s}^k, \tilde{v}^k, Y_{\text{upg}}(a), \quad (\text{U.4})$$

$$(4) \text{ for } \tilde{v}^k, I_{\max, \text{upg}}, \quad (\text{U.5})$$

$$\forall k \in \{1, \dots, K\}$$

where $a, \tilde{v}^k, \tilde{s}^k$ are optimization variables and the remaining symbols are given data. The cost function is chosen to be the sum of upgrades performed, but any convex cost function in a would be admissible. Problem (U), equivalently reformulated as an MI-QCQP with an added policy constraint, is

Problem P:

$$\underset{a, z^k, y^k}{\text{minimize}} \quad 1^T a \quad (\text{P.1})$$

$$\text{subject to} \quad a \in \{0, 1\}^{n_u}, \quad (\text{P.2})$$

$$Aa \leq b, \quad (\text{P.3})$$

$$Cy^k \leq d^k, \quad (\text{P.4})$$

$$\alpha_h \leq (z^k)^T Q_h z^k + q_h^T y^k + m_h^T a \leq \beta_h, \quad (\text{P.5})$$

$$(\tilde{s}^k, \tilde{v}^k) = g(a, \text{limits}^k) \quad (\text{P.6})$$

$$\forall h \in \{1, \dots, H\}, \forall k \in \{1, \dots, K\}.$$

The following sections outline the variable correspondences and how the constraints are brought into the standard form above. Problem (P) is non-convex due to the constraints in (P.5), the integrality constraints (P.2) and potentially the policy constraints (P.6). The latter have been rewritten to depend on a instead of Y_{upg} without loss of generality since Y_{upg} can be computed from a using (6).

3.2 Voltage magnitude constraints

A bus voltage magnitude constraint,

$$v_{\min, j} \leq |\tilde{v}_j^k| \leq v_{\max, j}, \quad (11)$$

can be rewritten as,

$$v_{\min, j}^2 \leq (v_{r, j}^k)^2 + (v_{q, j}^k)^2 \leq v_{\max, j}^2, \quad (12)$$

where the newly introduced variables $v_r^k, v_q^k \in \mathbb{R}^N$ represent the real and imaginary parts of \tilde{v}^k (separate vectors for each scenario k) and hence as,

$$v_{\min, j}^2 \leq (z^k)^T Q_j z^k \leq v_{\max, j}^2, \quad (13)$$

where we introduced the shorthand notation $z^k := [(v_r^k)^T \quad (v_q^k)^T]^T$ and where Q_j has entries equal to 1 in positions (j, j) and $(N + j, N + j)$ and zeros everywhere else. The constraint (13) is now in the form of (P.5).

3.3 Current constraints

A current constraint,

$$|Y_{\text{upg}, jl}| \cdot |\tilde{v}_j^k - \tilde{v}_l^k| \leq I_{\max, \text{upg}, jl}, \quad (14)$$

requires slightly more work to reformulate. We first move everything related to upgrades to the right-hand side and square both sides,

$$|\tilde{v}_j^k - \tilde{v}_l^k|^2 \leq \frac{I_{\max, \text{upg}, jl}^2}{|Y_{\text{upg}, jl}|^2}. \quad (15)$$

We then rewrite the left-hand side as a function of z ,

$$\begin{aligned} |\tilde{v}_j^k - \tilde{v}_l^k|^2 &= (v_{r, j}^k - v_{r, l}^k)^2 + (v_{q, j}^k - v_{q, l}^k)^2 \\ &= (z^k)^T Q_{jl} z^k, \end{aligned} \quad (16)$$

where now Q_{jl} is zero everywhere except entries 1 at $(j, j), (l, l), (N + j, N + j), (N + l, N + l)$ and entries -1 at $(j, l), (l, j), (N + j, N + l), (N + l, N + j)$. The right-hand side of (15) depends on the upgrade choices.

Recalling (6) and (8) and the fact that only one upgrade choice can be made for each line, the fraction in (15) can be rewritten as an equation that is linear in a ,

$$\frac{I_{\max, \text{upg}, jl}^2}{|Y_{\text{upg}, jl}|^2} = \frac{I_{\max, jl}^2}{|Y_{jl}|^2} + \sum_{i \in \mathcal{U}_{jl}} a_i \left[\left(\frac{\Delta I_{jl, i} + I_{\max, jl}}{|\Delta(Y_i)_{jl} + Y_{jl}|} \right)^2 - \frac{I_{\max, jl}^2}{|Y_{jl}|^2} \right]. \quad (17)$$

We can now write the line current constraints as

$$(z^k)^T Q_{jl} z^k + m_{jl}^T a \leq u_{jl}, \quad (18)$$

where $u_{jl} = I_{\max, jl}^2 / |Y_{jl}|^2$, and

$$(m_{jl})_i = - \left[\left(\frac{\Delta I_{jl, i} + I_{\max, jl}}{\Delta(Y_i)_{jl} + |Y_{jl}|} \right)^2 - \frac{I_{\max, jl}^2}{|Y_{jl}|^2} \right], \quad (19)$$

for $i \in \mathcal{U}_{jl}$ and 0 otherwise. Equation (18) now has the same structure as (P.5).

3.4 Line power constraints

The concept used to implement the line power constraints is similar to the one in [10]. We implement Big-M type constraints that select one out of several equalities depending on which upgrade is selected. We start from the power flow equations that each upgrade must satisfy,

$$\tilde{s}^k = \text{diag}(\tilde{v}^k) \overline{Y_{\text{upg}}(a)} \tilde{v}^k. \quad (20)$$

The products of binary and continuous variables in equality constraints will lead to non-convex relaxations. In order to avoid such products, we introduce separate case distinctions for each line as follows:

$$\tilde{s}_{jl}^k = \begin{cases} \tilde{v}_j^k \overline{Y_{\text{upg}, jl}(\hat{a}^1)} (\tilde{v}_l^k - \tilde{v}_j^k), & \text{if } a = \hat{a}^1 \\ \tilde{v}_j^k \overline{Y_{\text{upg}, jl}(\hat{a}^2)} (\tilde{v}_l^k - \tilde{v}_j^k), & \text{if } a = \hat{a}^2 \\ \vdots \\ \tilde{v}_j^k \overline{Y_{\text{upg}, jl}(\hat{a}^{n_u(jl)})} (\tilde{v}_l^k - \tilde{v}_j^k), & \text{if } a = \hat{a}^{n_u(jl)} \end{cases} \quad (21)$$

where \tilde{s}_{jl}^k is to be read as “power flowing into bus j , out of the line (j, l) ” and the individual \hat{a}^m , $m \in \{1, \dots, n_u(jl)\}$, are the different upgrade possibilities affecting the line (j, l) . The \tilde{s}_{jl}^k can be expressed using additional variables $f_r^k \in \mathbb{R}^{2L}$ and $f_q^k \in \mathbb{R}^{2L}$, which represent real and reactive powers flowing into buses from lines,

$$\tilde{s}_{jl}^k = (f_r)_{jl}^k + \sqrt{-1} \cdot (f_q)_{jl}^k. \quad (22)$$

In the above, the index jl is used to refer to the entries in f_r and f_q that are assigned to the real and reactive parts of the power flowing into bus j from the line between buses j and l . Note that while there can be many binary variables in the complete problem, the number of variables affecting a particular line is typically small. Additional constraints are needed to enforce the power balance for each bus,

$$\begin{aligned} p_{\min, j}^k &\leq \sum_l \text{Re}(\tilde{s}_{jl}^k) \leq p_{\max, j}^k, \\ q_{\min, j}^k &\leq \sum_l \text{Im}(\tilde{s}_{jl}^k) \leq q_{\max, j}^k, \end{aligned} \quad (23)$$

where the sum is over all neighboring indices l of j . All constraints for a scenario k of the kind in (23) are then collected in the constraints (P.4). As for the actual implementation, for a line (j, l) and upgrade option i affecting it, we introduce the notation $Y_{\text{upg}, jl}(a_i = 1)$ to refer to the admittance of line jl in case $a_i = 1$

(which, by the constraint that just one of the upgrades per line can be chosen, implies that all other entries of a with indices in \mathcal{U}_{jl} are zero). Using this notation, we would have the constraints

$$\begin{aligned} \left| (f_r^k)_{jl} - \operatorname{Re} \left(\tilde{v}_j^k \overline{Y_{\text{upg},jl}(a_i = 1)(\tilde{v}_l^k - \tilde{v}_j^k)} \right) \right| &\leq M_{jl}(1 - a_i), \\ \left| (f_q^k)_{jl} - \operatorname{Im} \left(\tilde{v}_j^k \overline{Y_{\text{upg},jl}(a_i = 1)(\tilde{v}_l^k - \tilde{v}_j^k)} \right) \right| &\leq M_{jl}(1 - a_i), \end{aligned} \quad (24)$$

where M is large enough that if $a_i = 0$, the two constraints can never be active for an otherwise feasible choice of the variables. The choice of M is important to good relaxation conditioning, which is why it is discussed in more detail in Section 3.5. In addition to the above, a “no upgrade to this line” case has to be added,

$$\begin{aligned} \left| (f_r^k)_{jl} - \operatorname{Re} \left(\tilde{v}_j^k \overline{Y_{jl}(\tilde{v}_l^k - \tilde{v}_j^k)} \right) \right| &\leq M_{jl} \sum_{i \in \mathcal{U}_{jl}} a_i, \\ \left| (f_q^k)_{jl} - \operatorname{Im} \left(\tilde{v}_j^k \overline{Y_{jl}(\tilde{v}_l^k - \tilde{v}_j^k)} \right) \right| &\leq M_{jl} \sum_{i \in \mathcal{U}_{jl}} a_i, \end{aligned} \quad (25)$$

where the summation over upgrade index i only includes the upgrades that affect the given line. The quadratic terms in (25) can be rewritten as follows:

$$\begin{aligned} \operatorname{Re} \left(\tilde{v}_j^k \overline{Y_{jl}(\tilde{v}_l^k - \tilde{v}_j^k)} \right) &= \\ &= -\operatorname{Re}(Y_{jl})(v_r^k)_j^2 + \operatorname{Re}(Y_{jl})(v_r^k)_j(v_r^k)_l \\ &\quad - \operatorname{Im}(Y_{jl})(v_r^k)_j(v_q^k)_l + \operatorname{Re}(Y_{jl})(v_q^k)_j(v_q^k)_l \\ &\quad - \operatorname{Re}(Y_{jl})(v_q^k)_j^2 + \operatorname{Im}(Y_{jl})(v_q^k)_j(v_r^k)_l, \\ \operatorname{Im} \left(\tilde{v}_j^k \overline{Y_{jl}(\tilde{v}_l^k - \tilde{v}_j^k)} \right) &= \\ &= \operatorname{Re}(Y_{jl})(v_q^k)_j(v_r^k)_l - \operatorname{Im}(Y_{jl})(v_q^k)_j(v_q^k)_l \\ &\quad + \operatorname{Im}(Y_{jl})(v_q^k)_j^2 - \operatorname{Re}(Y_{jl})(v_r^k)_j(v_q^k)_l \\ &\quad - \operatorname{Im}(Y_{jl})(v_r^k)_j(v_r^k)_l + \operatorname{Im}(Y_{jl})(v_r^k)_j^2. \end{aligned} \quad (26)$$

A similar procedure can be used for (24), simply by replacing Y_{jl} with $Y_{\text{upg},jl}(a_i = 1)$. This means the line power constraints are now quadratic in z^k and linear in $y^k := [(f_r^k)^T \ (f_q^k)^T]^T$ and a , as was required (the absolute value operator can simply be replaced with two linear constraints). The data for the Q terms is given in (26). The data for the q terms is determined by how the variables are ordered in f_r^k and f_q^k and by (24) and (25). The data for the m terms is also determined by (24) and (25). Each set of constraints in (24) or (25) translates into 4 constraints of the form (P.5) due to the absolute value involved.

3.5 Computation of Big-M terms for line powers

Problem (P) will later be solved in a Branch-and-Bound setting by relaxing the integrality constraints on a_i to be $a_i \in [0, 1]$. The constant M should be chosen large enough for (24)-(25) to implement (21), but should also be as small as possible to avoid numerical issues. For this reason, instead of a single M for all constraints, a separate constant M_{jl} is found for each line from bus j to bus l . The following Lemma gives a lower bound on M_{jl} .

Lemma 1. *In order for the case distinction (21) to be equivalent to the intersection of the constraints in (24) and (25), it has to hold that*

$$\begin{aligned} M_{jl} &\geq v_{\max,j} \max |\tilde{v}_l^k - \tilde{v}_j^k| \cdot \\ &\quad \max_{i_1, i_2 \in \mathcal{U}_{jl}} |Y_{\text{upg},jl}(a_{i_1} = 1) - Y_{\text{upg},jl}(a_{i_2} = 1)|, \end{aligned} \quad (27)$$

where the term $\max |\tilde{v}_l^k - \tilde{v}_j^k|$ refers to the maximum absolute value of the difference between \tilde{v}_l^k and \tilde{v}_j^k that can occur in scenario k .

Proof. For any integral choice of a satisfying (7), one of the cases in (21) is selected by means of the right hand side of one of the corresponding constraints in (24)–(25) becoming 0. This is referred to hereafter as this constraint being *active*. What is to be shown is that if M_{jl} is chosen to satisfy (27), none of the other constraints in (24)–(25) can be violated for any admissible choice of \tilde{v}^k . For this, the largest absolute value that any of the non-active constraints can attain is to be found and then M_{jl} has to be picked larger than that. We first define a shorter version of the notation introduced after (23),

$$y_{jl}(i) := Y_{\text{upg},jl}(a_i = 1),$$

as well as a shorthand notation for the difference between voltages of two buses j and l , $\Delta\tilde{v}_{jl}^k := \tilde{v}_j^k - \tilde{v}_l^k$. We can then write the largest possible absolute value as

$$\begin{aligned} & \max_{i_1, i_2} \max_{\tilde{v}^k} \left| \operatorname{Re} \left(\tilde{v}_j^k \overline{y_{jl}(i_1) \Delta\tilde{v}_{lj}^k} \right) - \operatorname{Re} \left(\tilde{v}_j^k \overline{y_{jl}(i_2) \Delta\tilde{v}_{lj}^k} \right) \right| \\ & \leq \max_{i_1, i_2} \max_{\tilde{v}^k} \left| \tilde{v}_j^k (y_{jl}(i_1) - y_{jl}(i_2)) \Delta\tilde{v}_{lj}^k \right| \\ & = \max_{\tilde{v}^k} |\tilde{v}_j^k| \max_{\tilde{v}^k} |\Delta\tilde{v}_{lj}^k| \max_{i_1, i_2} |y_{jl}(i_1) - y_{jl}(i_2)|. \end{aligned} \quad (28)$$

The first term in the last row above is just $v_{\max,j}$ from the problem data. The last line of the above therefore equals (27), which completes the proof. \square

The last term in (27) can easily be evaluated exactly by enumeration of the possible pairs of different line parameters. A bound on $\Delta\tilde{v}_{lj}^k$ is supplied by the current limits through (15). In order to get a bound that holds for all possibilities, a maximization over a is performed.

$$\Delta\tilde{v}_{lj}^k = |\tilde{v}_l^k - \tilde{v}_j^k|^2 \leq \max_a \frac{I_{\max, \text{upg}, lj}^2(a)}{|Y_{\text{upg}, lj}(a)|^2}. \quad (29)$$

4 Algorithm

In order to solve (P), a Branch-and-Bound procedure augmented with constraint generation is applied to its mixed-integer semidefinite relaxation. This relaxation has the form

$$\begin{aligned} & \underset{\substack{a, Z^k, y^k \\ k \in \{1, \dots, K\}}}{\text{minimize}} \quad 1^T a \end{aligned} \quad (\text{R.1})$$

$$\text{subject to } a \in \{0, 1\}^{n_u}, \quad (\text{R.2})$$

$$Aa \leq b, \quad (\text{R.3})$$

$$Cy^k \leq d^k, \quad (\text{R.4})$$

$$\alpha_h \leq \operatorname{tr}(Q_h Z^k) + q_h^T y^k + m_h^T a \leq \beta_h, \quad (\text{R.5})$$

$$Z^k \succeq 0, \quad (\text{R.6})$$

$$\forall h \in \{1, \dots, H\}, \forall k \in \{1, \dots, K\}.$$

Problem (R) is a relaxation of (P): The policy constraints are removed and the non-convex quadratic constraints are replaced by a semidefinite relaxation. This algorithm was presented in [15] along with a proof that it solves (P). It will be extended here to work in concert with the Benders decomposition.

4.1 Benders decomposition

Note that the convex problems formed by relaxing the integrality constraints in (R) require one semidefinite variable Z^k as well as one vector of auxiliary variables y^k for each scenario k . The full set of power flow constraints and the operational constraints also need to be added separately for each of these scenarios. For $K \gg 1$, problem (R) becomes difficult to handle in a centralized manner.

The generalized Benders decomposition [16, 17] provides an approach for dealing with such structured problems efficiently. For a problem of the form

$$\begin{aligned} & \underset{\xi, \zeta}{\text{minimize}} \quad F(\zeta) \\ & \text{subject to} \quad G(\xi, \zeta) \leq 0, \quad \xi \in \mathcal{X}, \zeta \in \mathcal{Z}, \end{aligned} \quad (31)$$

with $F, G, \mathcal{X}, \mathcal{Z}$ convex, the method provides an algorithm that alternately fixes one of ζ and ξ while solving the problem for the other. The minimization with respect to ζ is referred to as the “master problem”, defined as follows:

Problem M:

$$\underset{\zeta}{\text{minimize}} \quad F(\zeta) \quad (M.1)$$

$$\text{subject to} \quad \min_{\xi \in \mathcal{X}} \{\lambda^T G(\xi, \zeta)\} \leq 0, \quad \forall \lambda \in \Lambda, \quad (M.2)$$

$$\zeta \in \mathcal{Z}. \quad (M.3)$$

where Λ is a set of vectors which will be iteratively built in the algorithm. Conversely, the minimization for ξ is referred to as the “subproblem” and defined as

Problem S:

$$\underset{\xi, \gamma \in \mathbb{R}}{\text{minimize}} \quad \gamma \quad (S.1)$$

$$\text{subject to} \quad G(\xi, \zeta) \leq 1\gamma, \quad (S.2)$$

$$\xi \in \mathcal{X}. \quad (S.3)$$

The full Benders decomposition algorithm is now stated in Figure 1, and the interested reader is referred to [16, 17] for more discussion. Each iteration of the algorithm either finds the optimal solution to (31) or improves the lower bound on the optimal cost. The Benders iteration can hence be stopped at any point and the lower bound obtained at that point is valid. This makes the algorithm particularly suitable for solving relaxations in a Branch-and-Bound procedure. In our application, we partition the variables of Problem (R) as

$$\xi^k := (Z^k, y^k), \quad \zeta := a. \quad (34)$$

We refer to the collection of ξ^k for $k \in \{1, \dots, K\}$ as ξ . We can then define the sets \mathcal{X} and \mathcal{Z} :

$$\begin{aligned} \mathcal{X}^k &:= \left\{ (Z^k, y^k) \mid \begin{array}{l} Cy^k \leq d^k \\ Z^k \succeq 0 \end{array} \right\}, \quad \forall k \in \{1, \dots, K\}, \\ \mathcal{X} &:= \bigcap_{k=1}^K \mathcal{X}^k, \end{aligned} \quad (35)$$

and

$$\mathcal{Z} := \left\{ a \mid \begin{array}{l} a \in [0, 1]^{n_u} \\ Aa \leq b \end{array} \right\}. \quad (36)$$

Additionally, those constraints in (R.5) that correspond to the voltage magnitude constraints (3) can also be added to \mathcal{Z} since they do not depend on a . The rest of the constraints in (R.5) are now stacked to make $G^k(\xi, \zeta)$:

$$G^k(\xi^k, \zeta) := \begin{bmatrix} -\text{tr}(Q_1 Z^k) - q_1^T y^k - m_1^T a + \alpha_1 \\ \text{tr}(Q_1 Z^k) + q_1^T y^k + m_1^T a - \beta_1 \\ -\text{tr}(Q_2 Z^k) - q_2^T y^k - m_2^T a + \alpha_2 \\ \text{tr}(Q_2 Z^k) + q_2^T y^k + m_2^T a - \beta_2 \\ \vdots \end{bmatrix}, \quad (37)$$

and the $G^k(\xi^k, \zeta)$ are in turn stacked to make $G(\xi, \zeta)$. We note here that the constraint data Q_h, q_h, m_h, α_h and β_h are the same for all scenarios. Because the entries of $G(\xi, \zeta)$ are linear in a , the maximization for ξ in (M.2) can be performed independently of ζ by solving a semidefinite problem. The resulting constraints are linear in ζ and independent of ξ , making (M) a linear problem in ζ . Subproblem (S) becomes a semidefinite problem due to \mathcal{X} .

4.1.1 Decomposition of Benders subproblem

The main computational burden lies in solving the subproblem (S) as well as the parametric maximizations in (M.2). We will now discuss how these two problems can be solved in a separable manner. Consider the K individual problems,

Problem S^k :

$$\underset{\xi^k, \gamma^k \in \mathbb{R}}{\text{minimize}} \quad \gamma^k \tag{S^k.1}$$

$$\text{subject to} \quad G^k(\xi^k, \zeta) \leq 1\gamma^k, \tag{S^k.2}$$

$$\xi^k \in \mathcal{X}^k. \tag{S^k.3}$$

The optimal results $(\gamma^k)^*, (\xi^k)^*$ of these problems can be used to construct an optimal solution for problem (S). It holds that

$$\gamma^* = \max_k (\gamma^k)^* \tag{39}$$

where γ^* denotes the optimal γ for (S). The $(\xi^k)^*$ are feasible for (S) with the above choice of γ^* as well. The dual multipliers, however, are different. The complementarity conditions for constraint (S.2) can be written as

$$\lambda_k^T (G^k(\xi^k, \zeta) - 1\gamma) = 0, \quad k \in \{1, \dots, K\} \tag{40}$$

due to all the involved terms being non-negative. Hence for a given choice of optimal variables, it will hold that $\lambda_k = 0$ for all constraints for which $G^k((\xi^k)^*, \zeta) < 1\gamma^*$. Considering that $(\gamma^k)^* \geq \gamma^*$, let \mathcal{K} be defined as

$$\mathcal{K} := \{k \in 1, \dots, K \mid G^k((\xi^k)^*, \zeta) = \gamma^*\}. \tag{41}$$

For the optimal multipliers λ^k of (S), it holds that

$$\lambda^k = 0 \quad \forall k \notin \mathcal{K} \tag{42}$$

due to (40). In order to obtain the λ_k for the $k \in \mathcal{K}$, a reduced version of (S) can be solved where G is constructed from only the scenarios in \mathcal{K} . Note that in practice, $|\mathcal{K}| \ll |K|$, in fact it is exceedingly unlikely that $|\mathcal{K}| > 1$ occurs. If $|\mathcal{K}| = 1$, the individual λ_k for the single k in \mathcal{K} can be used as is, with all the others set to 0.

4.1.2 Decomposition of the parametric cut problem

The constraints (M.2) are parametrically solved in ξ once for each λ added to Λ . Due to the structure of G , the parametric problem can be written as follows:

$$\begin{aligned} \min_{\xi \in \mathcal{X}} \{ \lambda^T G(\xi, \zeta) \} &= \min_{\xi^k \in \mathcal{X}^k} \left\{ \sum_{k=1}^K \lambda_k^T G^k(\xi^k, \zeta) \right\} \\ &= \sum_{k=1}^K \min_{\xi^k \in \mathcal{X}^k} \{ \lambda_k^T G^k(\xi^k, \zeta) \}, \end{aligned} \tag{43}$$

which means the parametric cut problems can be solved separately for each k and the results summed up.

```

1: Initialize  $\Lambda = \emptyset$ 
2: while No feasible solution  $\zeta$  found do
3:   Solve (M) for  $\zeta$  (solution:  $\zeta^*$ )
4:   Solve (S) for  $\xi$  with  $\zeta$  fixed to  $\zeta^*$  (solution:  $\xi^*, \gamma^*$ )
5:   if  $\gamma^* \leq 0$  then
6:     Stop,  $\xi^*, \zeta^*$  are optimal for (31)
7:   else
8:     Let  $\lambda^*$  be the dual multipliers of constraints (S.2)
9:     Add  $\lambda^*$  to  $\Lambda$ 
10:  end if
11: end while

```

Fig. 1: Benders decomposition algorithm for problems of the form (31). Intuitively speaking, the algorithm picks the best ζ possible without considering ξ using (M), then attempts to find a ξ that is still feasible using (S). If that fails, the information from (S) is used to restrict the search space in ζ .

4.2 Combined Branch-and-Bound and Benders algorithm

The modified Branch-and-Bound algorithm is shown in Figure 2, extended to include the changes introduced by the application of the Benders decomposition for the relaxations. The major differences to the version presented in [15] are as follows:

- 1) The relaxations are solved with the Benders decomposition. Only a limited number, $B \in \mathbb{N}$, of Benders iterations are performed on each relaxation.
- 2) The algorithm reuses cuts obtained from the partial solves for tightened versions of the relaxation from which they were obtained, since they remain valid.

Heuristic methods include approaches such as the ones outlined in the introduction. Well-performing heuristics can lead to good or even optimal solutions being found very rapidly, even though the solution process will typically take a much longer time to certify that an optimal solution is actually optimal.

The following Lemmas provide an explanation as to why this combination of algorithms is computationally correct in the sense that no feasible points are artificially discarded.

Lemma 2. *Despite not solving the relaxed problems fully, the algorithm never cuts branches of the tree that would not have been cut if the relaxations were fully solved.*

Proof. Each Benders iteration yields a valid lower bound on the objective, $L_{\text{Benders}} \leq L_{\text{true}}$. This means that for the result of each iteration,

$$L_{\text{Benders}} > U \implies L_{\text{true}} > U,$$

and hence the branch cutting criterion can never discard a branch that should have been explored. \square

Lemma 3. *Cuts obtained in each Benders solve are valid for all descendants of that node in the Branch-and-Bound tree.*

Proof. The feasible set of each node is a restriction of that of all its parents. All constraints that were valid for the parent feasible set are also valid for the more restricted feasible set of the node itself. \square

Lemma 3 does not make a statement about whether the lower bound of the relaxations eventually reaches the true lower bound. While this is not explored further in this work, the numerical experiments suggest that the obtained lower bounds approximate the true values well enough for the algorithm to be effective.

- 1: Set $U = \infty, L = -\infty$, Tree: Root vertex $\mathcal{I}_0 = \mathcal{I}_1 = \emptyset$
- 2: **while** $U - L > \varepsilon$ **do**
- 3: Pick an unprocessed vertex \mathcal{N} with index sets $\mathcal{I}_0^{\mathcal{N}}, \mathcal{I}_1^{\mathcal{N}}$
- 4: Perform at most B benders iterations on (R) with (R.2) replaced by

$$a_i \in \begin{cases} \{0\}, & \text{if } i \in \mathcal{I}_0^{\mathcal{N}}, \\ \{1\}, & \text{if } i \in \mathcal{I}_1^{\mathcal{N}}, \\ [0, 1] & \text{otherwise.} \end{cases}$$

and the Benders cuts from all ancestors added

- 5: **if** Problem in step 4 was not infeasible **then**
- 6: Store the obtained Benders cuts in this node
- 7: Let $(a^{\mathcal{N}}, Z^{\mathcal{N}}, y^{\mathcal{N}})$ refer to the Benders result
- 8: Let $L^{\mathcal{N}} = 1^T a^{\mathcal{N}}$
- 9: **if** Feasible, $L^{\mathcal{N}} < U$ and $a^{\mathcal{N}} \in \{0, 1\}^{n_u}$ **then**
- 10: Evaluate policy $g(a^{\mathcal{N}}, \text{limits}^k), \forall k$
- 11: **if** Feasible for all k **then**
- 12: Update $U = 1^T a^{\mathcal{N}}$
- 13: **else**
- 14: Add cut $\|a - a^{\mathcal{N}}\|_1 \geq 1$
- 15: Go back to the solve step (line 4)
- 16: **end if**
- 17: **else if** $L^{\mathcal{N}} < U$ but $a^{\mathcal{N}} \notin \{0, 1\}^{n_u}$ **then**
- 18: Select index $\ell, \ell \notin \mathcal{I}_0^{\mathcal{N}} \cup \mathcal{I}_1^{\mathcal{N}}$
- 19: Add a vertex with $\mathcal{I}_0 = \mathcal{I}_0^{\mathcal{N}} \cup \{\ell\}, \mathcal{I}_1 = \mathcal{I}_1^{\mathcal{N}}$
- 20: Add a vertex with $\mathcal{I}_0 = \mathcal{I}_0^{\mathcal{N}}, \mathcal{I}_1 = \mathcal{I}_1^{\mathcal{N}} \cup \{\ell\}$
- 21: **end if**
- 22: **else**
- 23: Set lower bound for this subtree to ∞
- 24: **end if**
- 25: Update $L = \min \{L^{\mathcal{N}} \mid \mathcal{N} \in \text{tree}\}$
- 26: Run heuristic methods
- 27: **if** Heuristic methods yield feasible solution **then**
- 28: Update U to reflect best solution found
- 29: **end if**
- 30: **end while**

Fig. 2: Branch-and-Bound algorithm with policy constraint generation. The algorithm traverses the binary tree based on fixing entries a_i to either 1 or 0, relaxing the non-fixed entries to $[0, 1]$. The first difference between regular Branch-and-Bound and the algorithm here is the policy evaluation and constraint addition. See [15] for further details. The second difference is the application of incomplete Benders iterations for the relaxations, which is discussed in the text.

5 Numerical experiments

For the software implementation of the experiments in this section, the Julia language [18] was used in conjunction with the JuMP modeling package [19]. Semidefinite relaxations were solved with MOSEK, smooth nonlinear problems arising in the operating policy with IPOPT [20] and linear problems with Gurobi. The experiments were run on a machine with 64 GB of system memory and an AMD Ryzen 9 3950X (3.5 GHz). All experiments were performed in single-threaded mode. The operating system used was Debian Linux 10.

5.1 Experiment considerations

Both the centralized problem as well as the optimization problems in the Benders-based approach were solved using a single thread. This was done to make comparisons easier, such as comparing a single thread centralized solution to the Benders approach with 8 parallel workers. In practice, most numerical solver codes such as MOSEK can make use of multiple threads on the same machine and such parallelism can trivially be combined with the parallelism provided by the method presented here.

As mentioned in Lemma 2, the number of Benders iterations performed for a single relaxation can be chosen freely. Setting the iteration number high enough to ensure that all relaxations are solved to a high accuracy was deemed impractical since a large number of iterations would be required. On the other hand, setting a low maximum number of iterations leads to the lower bounds on the relaxation objective value being lower than the true relaxation objective. This in turn leads to an increase in the number of Branch-and-Bound nodes visited, because the tree can be cut less often. Experiments have shown that as few as between 3 and 10 Benders iterations per relaxation provide a good tradeoff between the time taken for each relaxation and the increase in the number of nodes visited by the Branch-and-Bound procedure due to the lower bounds being weaker.

One can hence say that the Branch-and-Benders approach makes sense in cases where the computation speed gained by increased parallelism is larger than the speed lost due to an increase in the number of nodes visited. While this statement is straightforward to understand and even quantify on a single problem instance, it is relatively challenging to generalize to a set of rules for when the method presented here makes sense. The approach taken here is to present an example that was small enough to run in a reasonable time frame on a single machine over a range of scenario numbers, discuss the results of this particular experiment and make some cautious extrapolation attempts based on the data.

5.2 Test problem instance

A realistic industrial case study was performed with part of the Zurich distribution grid. Actual load data was augmented with some simulated PV in-feeds. Additional studies on this data are given in [15]. Load data as well as the system topology data are the same as in [15], but only the strongest of the upgrade possibilities for a subset of lines is considered here to shorten computation times. A visual representation of the violations encountered for the system and load data is shown in Fig. 3. Different cardinality sets of randomly generated scenarios were used in the following experiments. The scenarios were created by perturbing a base scenario obtained from real load data. In the experiment presented here, the policy was simply solving an AC economic dispatch to local optimality using IPOPT.

A greedy heuristic based on adding one upgrade at a time was used to look for feasible solutions. This heuristic was run on every feasible relaxation encountered and was computationally rather expensive, as for each upgrade addition the operating policy is evaluated for each scenario separately. The greedy heuristic was also trivially parallelizable, however.

5.3 Runtime comparison

The runtimes for the centralized and Branch-and-Benders approaches are shown in Table 1. The column named “Benders 3/1” refers to a configuration where at most 3 Benders iterations were performed on each relaxation solve and everything runs in a single-threaded configuration. Similarly, “Benders 3/K” refers to a hypothetical implementation where K workers are used in parallel. The relaxation times are separated into two numbers in the Benders columns, the first being the subproblem time and the second being the

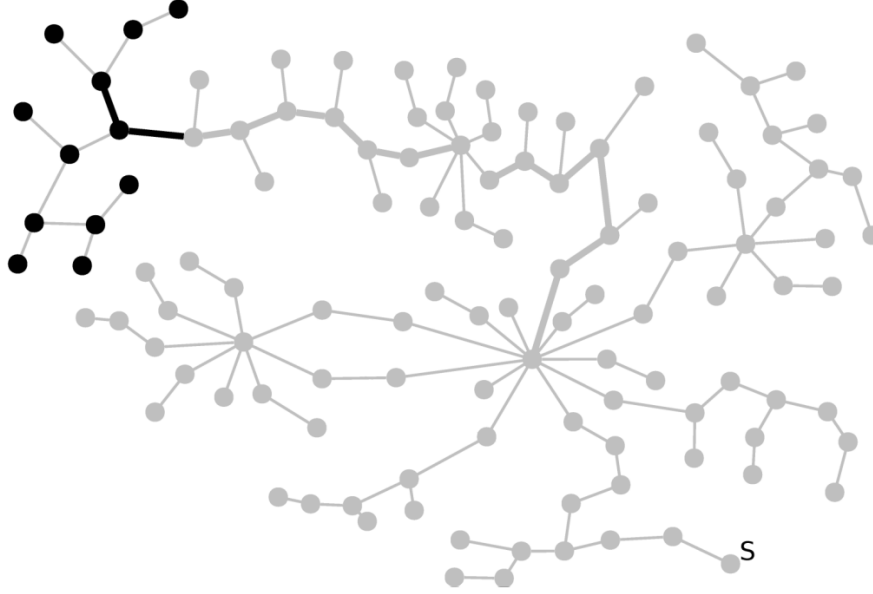


Fig. 3: Visualization of part of the Zurich distribution grid and violations encountered with a simulated load scenario. Dark vertices represent buses with voltage magnitude violations, dark lines represent current limit violations. The slack bus is denoted by “S”. The thicker lines represent lines that are considered for upgrades in the study.

sum of the master and cut problem times. For the computation of the runtimes in the parallel scenario, the subproblem time was divided by the number of agents K and 10% was added to the result to account for communication overhead that a real implementation would have. The cut and master problem times were taken as they are, because no parallelisation is suggested in the method here for them. Similarly, the time for the heuristics and policy checks was divided by the number of agents and 10% was added to the resulting time for coordination.

Investigating the data, one can see that for a single scenario the Benders-based approach makes little sense — the overhead that stems from having to solve multiple Benders iterations combined with more nodes being visited leads to a much worse overall runtime. For 20 scenarios, the situation is different. While taking the Branch-and-Benders approach with a single thread still takes more than twice the time as solving the centralized problem, the Benders approach scales very well with the number of parallel processing agents. For the best case of having as many processing agents as there are scenarios, the Benders approach winds up using less than 18% of the runtime of the centralized approach, despite visiting more than twice as many nodes.

This result is of course optimistic in some aspects: The centralized approach is expected to also scale well if the numerical solver used is given more threads to work with, and the parallelization of both heuristics and policy checks can be done independently of how the relaxations are solved. Regardless, a problem of real scale may have thousands of scenarios, growing the gap between a centralized solution with a many-core machine and the Benders approach with dozens or even hundreds of machines at its disposal. Note that this is not because the Benders approach is inherently more computationally efficient, but because it allows the computation to be distributed across a large set of computers. As mentioned earlier, additional forms of parallelization such as solving individual subproblems with multiple threads or examining multiple Branch-and-Bound tree nodes concurrently can be combined with what is presented here without any issues.

5.4 Discussion of runtime behavior

In order to aid potential users of the method decide whether it makes sense for their problem scale, this section will discuss the expected behavior of runtimes based on small-scale experiments with 1, 5, 10, 15 and 20 scenarios. In Figure 4, graphs are shown comparing the first and third solution methods listed in Table 1

Table 1: Comparison of centralized and Benders solve times

1 scenario	centralized	Benders 3/1	Benders 3/K
Final objective:	3	3	3
Nodes visited:	6	14	14
Policy cuts:	1	1	1
Policy checks [s]:	1.8	1.8	1.8
Heuristics [s]:	8.5	19.5	19.5
Relaxations [s]:	18.8	56.8 + 29.0	56.8 + 29.0
Total time [s]:	29.1	107.1	107.1
20 scenarios	centralized	Benders 3/1	Benders 3/K
Final objective:	4	4	4
Nodes visited:	42	86	86
Policy cuts:	36	14	14
Policy checks [s]:	693.9	277.0	15.2
Heuristics [s]:	1460.4	3333.5	183.3
Relaxations [s]:	2043.1	6974.6 + 145.5	383.6 + 145.5
Total time [s]:	4197.5	10730.6	727.7

for these numbers of scenarios.

In the upper plot, it can be seen that the computational advantage steadily increases with the number of scenarios. This behavior is expected, because for the best case of as many agents as there are scenarios, the time per Benders iteration is roughly constant, whereas the centralized solution time grows at least linearly with the number of scenarios. In the lower plot, total runtimes are shown for comparison, though care has to be taken when showing absolute times for different scenario numbers in the same plot. This is because the Branch-and-Bound trees, number of heuristic evaluations and number of nodes visited vary across the different scenario counts.

These experiments showed quite regular behavior, because they all required only 3 to 4 upgrades to the system and hence required only a slowly growing number of nodes to be visited as more scenarios were added. If more scenarios are added or a different power system is optimized over, the number of upgrades required can become higher and with that the runtime of both the centralized and parallel approaches can grow substantially. However, as long as the number of nodes required for Benders does not grow strongly compared to the number of nodes required for the centralized approach, the advantage gained due to the Benders-based parallelization is expected to persist and even grow with an increasing number of scenarios.

In Figure 5, timings are shown for a single relaxation instead, but up to 200 scenarios. The Benders times were scaled to 10 iterations for the experiment. For a problem with 200 scenarios, 10 iterations of Benders implementation with 16 parallel agents would outperform the centralized approach by more than an order of magnitude. For a fully parallel implementation, the performance gap would even grow to two orders of magnitude.

6 Conclusion

This work presents an algorithmic framework for effectively solving power system line upgrade problems at a scale applicable to many city distribution networks. The method deterministically finds globally optimal solutions provided they exist, and certificates that they do not otherwise. The use of the Benders decomposition for solving relaxations renders the core computational burden of the algorithm parallelizable to a large extent.

While more research is needed regarding the impact of weaker lower bounds on individual relaxations due to incomplete Benders iterations on a wider class of problems, the numerical experiments presented

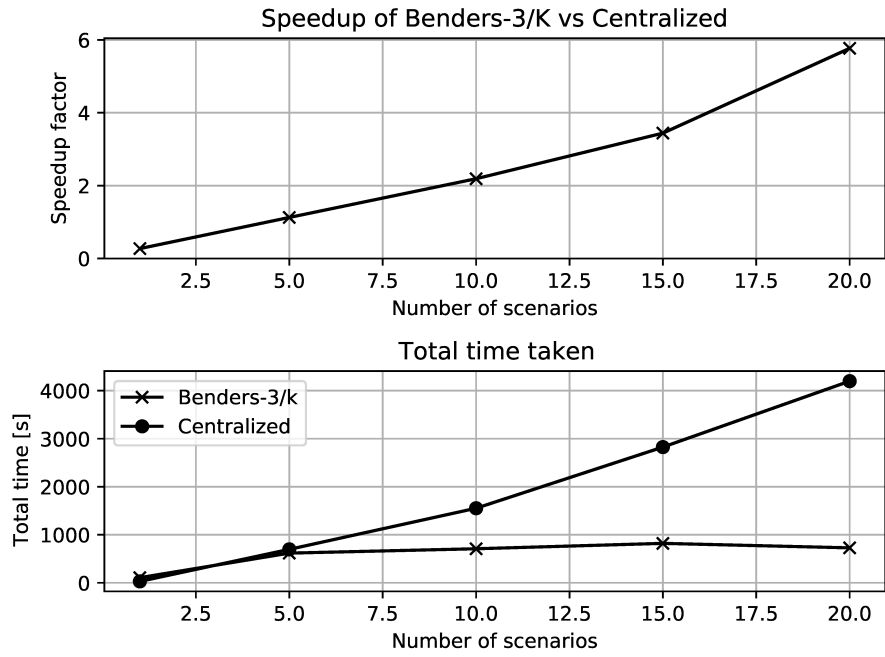


Fig. 4: Comparison of complete solve runtimes of centralized and fully parallel Benders approach for a series of scenario numbers.

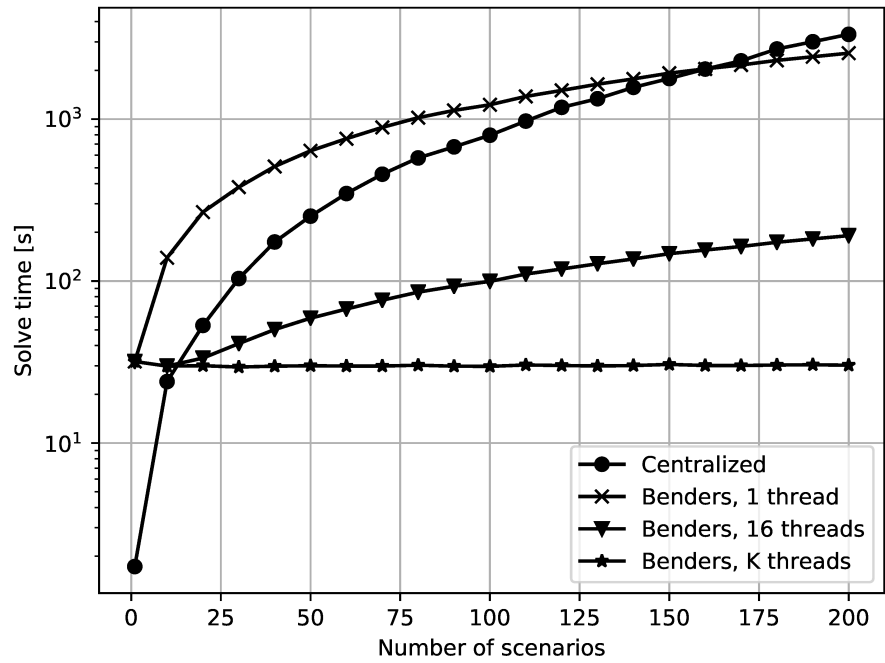


Fig. 5: Comparison of runtimes of a single relaxation using the centralized, Benders with 16 parallel computing agents and fully parallel (K agents) Benders methods

show that the Branch-and-Benders approach promises significant time savings for problems involving many scenarios.

In combination with more traditional parallelization avenues mentioned in the text, the Branch-and-Benders approach clears the way for future high-performance implementations on cluster computers.

7 Acknowledgments

This work was supported by the Swiss Commission for Technology and Innovation (CTI), (Grant 16946.1 PFIW-IW). We thank the team at Adaptricity (Stephan Koch, Andreas Ulbig, Francesco Ferrucci) for providing the system data and valuable discussions on power systems.

References

- [1] REN21, “Renewables 2015: Global status report,” [Online]. Available: <http://www.ren21.net/>, 2015.
- [2] H. Ayres, W. Freitas, M. D. Almeida, and L. D. Silva, “Method for determining the maximum allowable penetration level of distributed generation without steady-state voltage violations,” *IET Generation, Transmission & Distribution*, vol. 4, pp. 495–508(13), April 2010.
- [3] S. Merkli, A. Domahidi, J. L. Jerez, M. Morari, and R. S. Smith, “Fast AC Power Flow Optimization Using Difference of Convex Functions Programming,” *IEEE Trans. on Power Systems*, vol. 33, no. 1, pp. 363–372, 2018.
- [4] K. Lehmann, A. Grastien, and P. V. Hentenryck, “AC-Feasibility on Tree Networks is NP-Hard,” *IEEE Trans. on Power Systems*, vol. 31, no. 1, pp. 798–801, 2016.
- [5] M. J. Rider, A. V. Garcia, and R. Romero, “Power system transmission network expansion planning using AC model,” *IET Generation, Transmission Distribution*, vol. 1, no. 5, pp. 731–742, 2007.
- [6] I. J. Ramirez-Rosado and J. L. Bernal-Agustin, “Genetic algorithms applied to the design of large power distribution systems,” *IEEE Trans. on Power Systems*, vol. 13, no. 2, pp. 696–703, 1998.
- [7] L. H. Macedo, C. V. Montes, J. F. Franco, M. J. Rider, and R. Romero, “An MILP Branch Flow Model for Concurrent AC Multistage Transmission Expansion and Reactive Power Planning with Security Constraints,” *IET Generation, Transmission & Distribution*, vol. 10, pp. 3023–3032, 2016.
- [8] S. H. Low, “Convex Relaxation of Optimal Power Flow - Part II: Exactness,” *IEEE Trans. Control of Network Systems*, vol. 1, no. 2, pp. 177–189, 2014.
- [9] L. Gan and S. H. Low, “Convex Relaxations and Linear Approximation for Optimal Power Flow in Multiphase Radial Networks,” in *2014 Power Systems Computation Conf.*, pp. 1–9, Aug 2014.
- [10] R. A. Jabr, “Optimization of AC transmission system planning,” *IEEE Trans. on Power Systems*, vol. 28, no. 3, pp. 2779–2787, 2013.
- [11] N. C. Koutsoukis, P. S. Georgilakis, and N. D. Hatziargyriou, “A tabu search method for distribution network planning considering distributed generation and uncertainties,” in *Int. Conf. Probabilistic Methods Applied to Power Systems (PMAPS)*, pp. 1–6, July 2014.
- [12] P. M. Esfahani, T. Sutter, and J. Lygeros, “Performance bounds for the scenario approach and an extension to a class of non-convex programs,” *IEEE Transactions on Automatic Control*, vol. 60, no. 1, pp. 46–58, 2015.
- [13] M. C. Campi and S. Garatti, “Wait-and-judge scenario optimization,” *Mathematical Programming*, vol. 167, no. 1, pp. 155–189, 2018.
- [14] G. C. Calafiore and M. C. Campi, “The scenario approach to robust control design,” *IEEE Transactions on Automatic Control*, vol. 51, no. 5, pp. 742–753, 2006.

- [15] S. Merkli, A. Domahidi, J. Jerez, and R. S. Smith, “Globally Optimal AC Power System Upgrade Planning under Operational Policy Constraints,” in *European Control Conf. (ECC)*, pp. 131–136, IEEE, 2018.
- [16] J. F. Benders, “Partitioning procedures for solving mixed-variables programming problems,” *Numerische Mathematik*, vol. 4, no. 1, pp. 238–252, 1962.
- [17] A. M. Geoffrion, “Generalized Benders Decomposition,” *J. Optimization Theory and Applications*, vol. 10, no. 4, pp. 237–260, 1972.
- [18] J. Bezanson, A. Edelman, S. Karpinski, and V. B. Shah, “Julia: A fresh approach to numerical computing,” *SIAM Review*, vol. 59, no. 1, pp. 65–98, 2017.
- [19] I. Dunning, J. Huchette, and M. Lubin, “JuMP: A Modeling Language for Mathematical Optimization,” *SIAM Review*, vol. 59, no. 2, pp. 295–320, 2017.
- [20] A. Wächter and L. T. Biegler, “Line search filter methods for nonlinear programming: Motivation and global convergence,” *SIAM J. Optimization*, vol. 16, no. 1, pp. 1–31, 2005.